



FY-23 Status Report on the Development of New ASME Section III, Division 5 Class B Rules

September 2023

Heramb Mahajan and Ting-Leung Sham
Idaho National Laboratory

Robert Jetter
SAS Consulting Group LLC

Yanli Wang
Oak Ridge National Laboratory



*INL is a U.S. Department of Energy National Laboratory
operated by Battelle Energy Alliance, LLC*

DISCLAIMER

This information was prepared as an account of work sponsored by an agency of the U.S. Government. Neither the U.S. Government nor any agency thereof, nor any of their employees, makes any warranty, expressed or implied, or assumes any legal liability or responsibility for the accuracy, completeness, or usefulness, of any information, apparatus, product, or process disclosed, or represents that its use would not infringe privately owned rights. References herein to any specific commercial product, process, or service by trade name, trade mark, manufacturer, or otherwise, does not necessarily constitute or imply its endorsement, recommendation, or favoring by the U.S. Government or any agency thereof. The views and opinions of authors expressed herein do not necessarily state or reflect those of the U.S. Government or any agency thereof.

FY-23 Status Report on the Development of New ASME Section III, Division 5 Class B Rules

**Heramb Mahajan and Ting-Leung Sham
Idaho National Laboratory
Robert Jetter
SAS Consulting Group LLC
Yanli Wang
Oak Ridge National Laboratory**

September 2023

**Idaho National Laboratory
Advanced Reactor Technologies
Idaho Falls, Idaho 83415**

<http://www.art.inl.gov>

**Prepared for the
U.S. Department of Energy
Office of Nuclear Energy
Under DOE Idaho Operations Office
Contract DE-AC07-05ID14517**

Page intentionally left blank

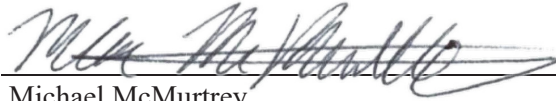
INL ART Program

**FY-23 Status Report on the Development of New
ASME Section III, Division 5 Class B Rules**

INL/RPT-23-74748

September 2023

Technical Reviewer: (Confirmation of mathematical accuracy, and correctness of data and appropriateness of assumptions.)



Michael McMurtrey
Materials Engineer

9/19/2023

Date

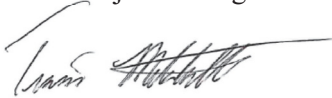
Approved by:



Michael E. Davenport
ART Project Manager

9/19/2023

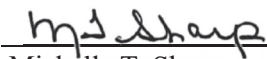
Date



Travis R. Mitchell
ART Program Manager

9/18/2023

Date



Michelle T. Sharp
INL Quality Assurance

9/19/2023

Date

Page intentionally left blank

SUMMARY

This report summarizes the work done in Fiscal Year 2023 on the development of the new American Society of Mechanical Engineers Boiler and Pressure Vessel Code, Section III, Division 5, Class B rules to address the gaps identified for high temperature reactor designs. The summary of the design-by-analysis strain limit evaluation and creep-fatigue damage assessment is presented. The proposed design-by-analysis creep-fatigue damage calculation approach uses a new elastic follow-up-based Isochronous Stress Strain Curve stress relaxation procedure. This approach captures the elastic follow-up generated due to interactions of components with adjacent components, supports, and other connections in the power plant. A set of sample problems are selected to validate the proposed design-by-analysis rules for creep-fatigue damage assessment. The proposed Class B rules are evaluated against the Class A elastic design rules and the experimental data obtained from a family of a simplified model test based key-feature test results. The proposed Class B creep-fatigue damage assessment methodology yields conservative design cycles estimates compared to the experimental results.

Page intentionally left blank

ACKNOWLEDGEMENTS

This research was sponsored by the U.S. Department of Energy (DOE) under Contract No. DE-AC07-05ID14517 with Idaho National Laboratory (INL), which is managed and operated by Battelle Energy Alliance, and under Contract No. DE-AC05-00OR22725 with Oak Ridge National Laboratory, which is managed and operated by UT-Battelle LLC.

Programmatic direction was provided by the Office of Nuclear Reactor Deployment of the DOE Office of Nuclear Energy (NE). The authors gratefully acknowledge the support provided by Sue Lesica of DOE-NE, Federal Materials Lead for the Advanced Reactor Technologies (ART) Program; Matthew Hahn of DOE-NE, Federal Program Manager of the ART Gas-Cooled Reactors (GCR) Campaign; and Gerhard Strydom of INL, ART GCR National Technical Director.

Page intentionally left blank

CONTENTS

SUMMARY	vii
ACKNOWLEDGEMENTS	ix
ACRONYMS	xiv
1. INTRODUCTION	1
2. DESIGN-BY-ANALYSIS METHODOLOGY	2
2.1 Strain Limits Evaluation and Check for Ratcheting	2
2.2 Creep-Fatigue Damage Assessment	3
3. EVALUATION OF THE PROPOSED DESIGN-BY-ANALYSIS CREEP-FATIGUE METHODOLOGY	6
3.1 Multiaxial Isothermal Tube	8
3.2 Single Bar Simplified Model Test	9
3.3 Pressurized Single Bar Simplified Model Test (p-SBSMT)	10
3.4 Pressurized Simplified Model Test (p-SMT)	11
3.5 Bree Problem	12
3.6 Flat Head Vessel	16
3.7 Influence of Primary Creep on the Class B Methodology	19
4. CANDIDATE CLASS B MATERIALS	23
5. SUMMARY AND FUTURE WORK	24
REFERENCE	25

FIGURES

Figure 1. Diagram showing the elastic follow-up.	2
Figure 2. Flow chart of the proposed strain limits evaluation for the Class B code case.	3
Figure 3. Stress-strain path taken by the Class B methodology	4
Figure 4. Material independent creep-fatigue damage envelope adopted with the intersection point of (0.2,0.2).	5
Figure 5. Schematic representation of creep and fatigue damage fractions for the maximum allowable design cycle, shown with Line A, compared against a generic creep-fatigue damage envelope.	6
Figure 6. Comparison of (a) stress-strain data and (b) stress relaxation history from the Class B methodology against the SBSMT test data [6] from the first hysteresis loop until end of dwell time.	9
Figure 7. Comparison of (a) stress-strain data until the end of hold time and (b) stress relaxation history from the Class B with $q = 6$ against p-SBSMT test data SBAP4 [7].	10

Figure 8. Comparison of (a) stress-strain data until end of hold time and (b) stress relaxation history from the Class B with $q = 6$ against p-SBSMT test data SBAP5 [7].	11
Figure 9. Specimen geometry of the pressurized SMT [8].	12
Figure 10. (a) Bree problem schematics with the boundary conditions and (b) temperature load profile.	13
Figure 11. Normalized life comparison calculated by dividing the maximum design cycles from Class B by the design cycles from Class A elastic rules for the Bree problem with different load cases for (a) 316H and (b) Alloy 617.	15
Figure 12. Creep damage accumulated over one cycle from Class A elastic and Class B methodologies for the Bree problem with different load cases for (a) 316H and (b) Alloy 617.	16
Figure 13. FHV geometry with the temperature load history.	17
Figure 14. The total strain ranges from Class A elastic and Class B methodologies for FHV problem with different load cases.	18
Figure 15. Creep damage accumulated over one cycle from Class A elastic and Class B methodologies for FHV problem with different load cases.	18
Figure 16. Creep damage accumulated over one cycle from Class A elastic and Class B methodologies using the simplified ISSCs and the standard ISSCs for the Bree problem with different load cases.	21
Figure 17. Influence of the primary creep on the normalized life for the Bree problem with different load cases.	21
Figure 18. Creep damage accumulated over one cycle from Class A elastic and Class B methodologies with simplified and standard ISSCs for FHV problem with different load cases.	22

TABLES

Table 1. A summary of an example problem with the respective load cycles.	8
Table 2. Maximum allowable cycles from Class A elastic compared against the Class B rules and failure cycles from multiaxial tube experiment.	8
Table 3. Comparison of the maximum allowable design cycles from Class B against the failure cycles from the SBSMT experiment.	9
Table 4. Comparison of the failure cycles from the p-SBSMT experiment against the Class B maximum allowable design cycles for different load cases.	10
Table 5. Comparison of the maximum allowable design cycles from Class A elastic and Class B design methodology against the failure cycles from p-SMT tests.	12
Table 6. Maximum allowable design cycles comparison from proposed Class B against the Class A Elastic calculated from the creep-fatigue damage.	13
Table 7. Comparison of maximum allowable design cycles from Class A and Class B.	17
Table 8. Influence of the primary creep strain on the design cycles for the Bree problem.	20
Table 9. Influence of the primary creep strain on the design cycles for FHV.	22

Table 10. List of candidate materials identified for incorporation into the new Class B code case.	23
---	----

ACRONYMS

ART	Advanced Reactor Technologies
ASME	American Society of Mechanical Engineers
BPVC	Boiler and Pressure Vessel Code
DOE	Department of Energy
EPP	Elastic-Perfectly Plastic
FEA	Finite Element Analysis
FHV	Flat Head Vessel
FY	Fiscal Year
HBA	Subsection HB, Subpart A
HBB	Subsection HB, Subpart B
HCA	Subsection HC, Subpart A
HCB	Subsection HC, Subpart B
INL	Idaho National Laboratory
ISSC	Isochronous Stress Strain Curve
NE	Nuclear Energy
ORNL	Oak Ridge National Laboratory
p-SBSMT	Pressurized Single Bar Simplified Model Test
p-SMT	Pressurized Simplified Model Test
PSY	Pseudo Yield Stress
SBSMT	Single Bar Simplified Model Test

FY-23 Status Report on the Development of New ASME Section III, Division 5 Class B Rules

1. INTRODUCTION

The American Society of Mechanical Engineers (ASME) Boiler and Pressure Vessel Code (BPVC) Section III, Division 5 [1] governs design rules for high-temperature nuclear component construction. Section III, Division 5, defines the importance levels of different components based on the component functionality and required structural integrity assurance. Class A code rules are used when component failure consequences are significant. Class B code rules are used when component failure consequences are less significant. The code classes offer designers a choice of rules that provide a reasonable assurance of structural integrity and quality based on the selected importance level of a component.

Current design rules for Class A components are defined in the ASME BPVC Section III, Division 5, Subsection HB, Subpart A (HBA), for low-temperature cyclic service below the creep regime, and are defined in Subsection HB, Subpart B (HBB), for elevated-temperature cyclic service in the creep regime. Current Class B component construction rules are defined in the ASME BPVC Section III, Division 5, Subsection HC, Subpart A (HCA), for low temperature and in Subsection HC, Subpart B (HCB), for high temperature operations. The HBB rules for Class A welded construction guard against structural failure modes through the primary load, strain limits, creep-fatigue, and buckling check using the design-by-analysis approach. The HCB rules are essentially the same as the ASME BPVC Section I and Section VIII, Division 1, for power boilers and pressure vessels applications, respectively. Section I and Section VIII, Division 1, rules are based on the design-by-rules approach that cover vessel, pump, valve, and piping design, but there are not design provisions for strain limits and creep-fatigue for these components. In HCB, the design rules for vessel, pump, and valve are the same as those in Section I and Section VIII, Division 1, but some conservative rules are adopted for creep-fatigue design for piping.

The HCB design rules for Class B components do not support the design life concept, and the allowable stresses for the primary load design in the creep regime are based on the extrapolated creep properties to 100,000 hours. Therefore, component construction with different a design life is not addressed. Designers could use the Class A elevated-temperature design rules for Class B components. However, there are only six Class A materials in HBB, and the addition of new Class A materials could be time consuming if the desired design lifetimes are greater than 100,000 hours. This limits the use of Class A rules for Class B construction.

These gaps were addressed in the previous report [2] for Fiscal Year 2022 (FY 2022). A new approach was proposed to extrapolate the creep properties, from the same Class B creep database, to very long design lifetimes using larger time extrapolation factors as compared with those of Class B for 100,000 hours. A new design-by-analysis provision was introduced to address the creep-fatigue interaction using a new elastic follow-up modified, or q -modified, stress relaxation procedure. Figure 1 shows the stress-strain behaviors for different values of q . For a stress relaxation load case with a constant strain hold, $q = 1$. For a constant stress load case, $q = \infty$. A discussion on the determination of q is given in [2].

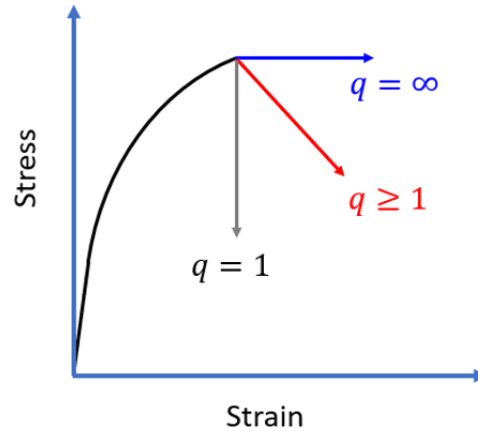


Figure 1. Diagram showing the elastic follow-up.

This report summarizes work conducted in FY 2023 on the development of the new Class B code case for components operating in the creep regime with the introduction of strain limits and creep-fatigue design-by-analysis provisions with a variable design lifetime. In consultation with industry stakeholders, a list of candidate Class B materials has been established to support the new advanced reactor designs. Data gaps for the new Class B rules are identified for the new Class B materials list. A new design-by-analysis approach for the strain limits evaluation using the Elastic, Perfectly Plastic (EPP) method with pseudo yield stress has been developed and discussed. A summary of the creep-fatigue damage evaluation procedure using the design-by-analysis is provided. A set of sample problems was used to evaluate the proposed Class B rules against the experimental results and the current Class A elastic analysis procedure. It was shown that the proposed Class B rules on assessing cyclic lives in the creep regime are conservative compared to the experimental data by an order of magnitude. The use of simplified isochronous stress-strain curves (ISSCs) that are based only on secondary creep was assessed against the standard ISSCs that include primary creep for 316H material on the creep-damage evaluation using the new Class B design rules.

2. DESIGN-BY-ANALYSIS METHODOLOGY

2.1 Strain Limits Evaluation and Check for Ratcheting

The proposed strain limits evaluation methodology is based on the ratcheting analysis. This approach uses a small strain theory with an EPP material properties, where the yield stresses are replaced by the pseudo yield stresses (PSYs). The flow chart for the proposed strain limits evaluation and ratcheting check is presented in Figure 2. This approach is similar to the strain limits evaluation approach employed in the EPP Code Case N-861-1 [3] for ASME BPVC Section III, Division 5, Class A construction [1].

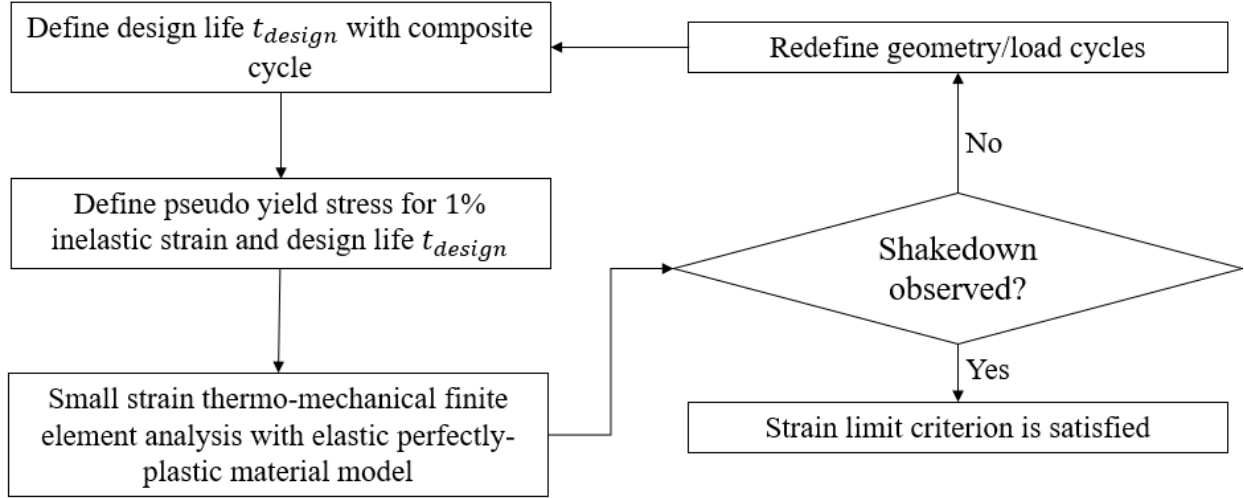


Figure 2. Flow chart of the proposed strain limits evaluation for the Class B code case.

The first step defines the design life with a composite cycle. In the second step, PSYs are defined as the minimum of the yield strength of the material and the time-temperature dependent stresses from the ISSCs based on the total time duration of high temperature service and a target inelastic strain of 1%. A small strain thermomechanical EPP finite element analysis (FEA) is conducted, where the yield stresses of material are replaced by time-temperature dependent PSYs. The analysis model uses a detailed component model geometry, including stress raisers with corner radii. To pass the strain limits check, strain history should achieve shakedown. Strain histories from all integration points are evaluated to check for shakedown. If shakedown is observed at all integration points, the component passes the strain limits check. If the component does not pass the strain limits check, load cycle, and component geometry are redefined, and all the steps are repeated until the strain limits check is satisfied.

2.2 Creep-Fatigue Damage Assessment

The creep-fatigue damage evaluation process involves the following steps.

1. Elastic analysis with all loads – Proposed Class B methodology does not rely on the stress classification. Thus, all loads (primary membrane stress + primary bending stress + peak stress + secondary stress) are accounted for directly to determine the maximum local stress. Temperature-dependent elastic material properties are used, which entail elastic moduli, Poisson's ratio, and thermal expansion coefficient. Thermo-mechanical FEA is conducted using component geometry. All features of the geometry, such as notch and stress concentration regions, are modeled in detail. This analysis provides stress histories at all integration points in the component for one cycle.
2. Peak stress calculation – Stress time histories from the FEA are used to calculate the peak stresses at all integration points per stress difference method in Section III Appendices, Mandatory Appendix XIII, XIII-2400 [4]. The maximum alternating stress intensity (S_{alt}) from all points is used to calculate the peak stress (σ_{peak}) as two times S_{alt} .
3. Stress relaxation – The elastically calculated peak stress (σ_{peak}) from step 2 is used as a starting point for the stresses to relax, as shown in Figure 3. The figure on the left side shows the ISSCs of the material at peak temperature, T , during the load cycle, and the figure on the right depicts the stress relaxation time history. For a given elastic follow-up, q , the stress is relaxed among the family of ISSCs along the slope $-\frac{E}{q-1}$, where E is the elastic modulus at peak temperature during the load

cycle. The point ‘a’ is the intersection of the elastic follow-up line and the hot-tensile curve. The stress is relaxed from S_a at point ‘a’ along the q -modified relaxation path, Line a–j in Figure 3, until the end of the dwell time t_{dwell} . For the calculation of the creep damage and the determination of the strain range for calculating the fatigue damage, the stress history during the dwell time is not allowed to fall below a lower bound stress, S_{LB} . The previous work established the equations for this step [2]. The equations listed below summarize the numerical approach.

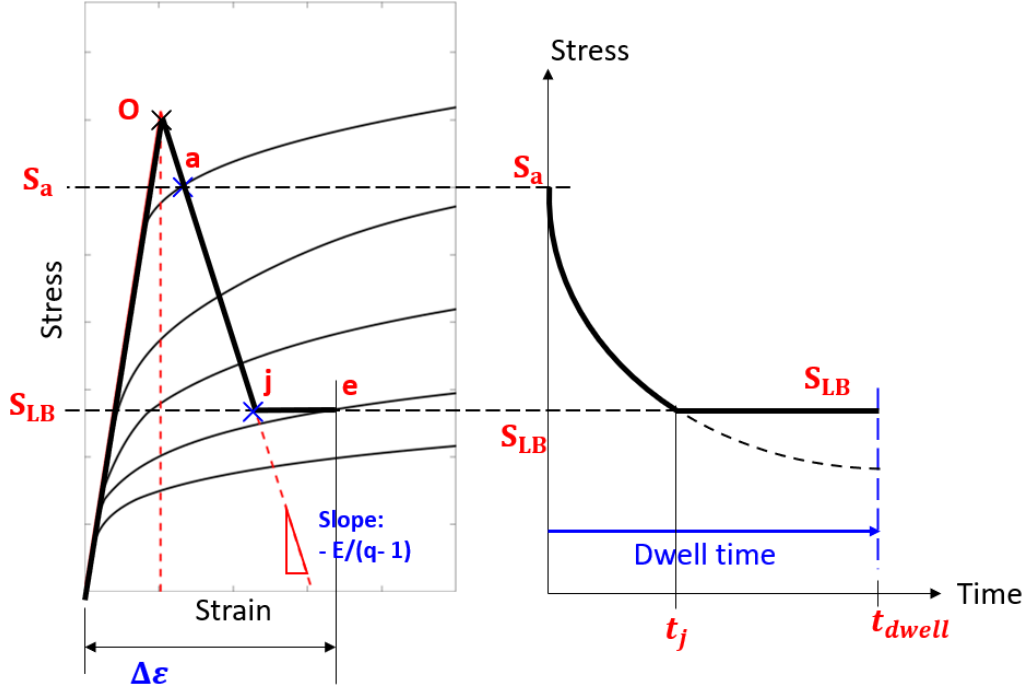


Figure 3. Stress-strain path taken by the Class B methodology shown in thick black lines on the ISSCs and the respective stress relaxation showing the total strain range used for fatigue damage calculation and the stress relaxation history for the creep damage.

The time required for the stress to relax from S_a to a value σ can be calculated from Equation 1a, where S_a is solved for numerically from the nonlinear algebraic equation in Equation 1b.

$$t = \frac{q}{E} \frac{\sigma_{peak} - \sigma}{\rho_s(\sigma)} - \frac{\varepsilon_{plastic}(\sigma)}{\rho_s(\sigma)} \quad \text{for } \sigma \leq S_a \quad \text{Eq. 1a}$$

$$S_a = \sigma_{peak} - \frac{E}{q} \varepsilon_{plastic}(S_a) \quad \text{Eq. 1b}$$

Here, $\varepsilon_{plastic}(\sigma)$ is the accumulated plastic strain and $\rho_s(\sigma)$ is the creep rate at stress σ . If σ_{peak} is at or below the yield stress of the material, the plastic strains in Equation 1a and Equation 1b are zero. The stress history used to determine the creep damage for the dwell period can be calculated numerically using Equation 2.

$$\sigma(t) = \max\left(\sigma_{peak} - \frac{E}{q} \rho_s(\sigma) t, S_{LB}\right) \quad \text{Eq. 2}$$

The next step provides a basis to calculate the lower bound stress, S_{LB} .

4. S_{LB} calculation – The stress relaxation does not go below a lower bound stress, S_{LB} , which is calculated as the pseudo yield stress for which the corresponding limit load equals the applied steady

state load. Conceptually, the lower bound stress limits the amount of stress relaxation during the dwell time, thus capturing the creep strain due to stresses originated from the steady state operation in the fatigue damage calculation.

5. Creep-fatigue damage – Once the required stress history during the dwell time is determined, the next step is to calculate the creep and fatigue damage fractions. The enhanced strain range, $\Delta\epsilon$, is the total strain range at the end of the dwell time, as shown in Figure 3. This strain range accounts for the elastically calculated strain due to the peak stress, the strain enhancement due to the stress relaxation along the q -modified path, and the creep strain accumulation due to the lower bound stress. Equation 3 provides a numerical approach to calculate the enhanced strain range.

$$\Delta\epsilon = \frac{q}{E}\sigma_{peak} - \frac{q-1}{E}\sigma(t_{dwell}) + \langle t_{dwell} - t_j \rangle \times \rho_s(S_{LB}) \quad \text{Eq. 3}$$

where $\sigma(t_{dwell})$ is determined from Equation 2, and $\rho_s(S_{LB})$ is the creep rate at S_{LB} . The first two terms provide the strain at point ‘j’ of Figure 3, and the third term accounts for the creep strain accumulation at the lower bound stress S_{LB} . The Macaulay bracket $\langle \ \rangle$ in the third term indicates that this term is needed only when the dwell time exceeds the time t_j of Figure 3. The total strain range $\Delta\epsilon$ from Equation 3 is used to calculate the number of cycles to failure (N_d) from the fatigue design curves. The fatigue damage fraction for design cycles n is calculated using Equation 4.

$$d_f = \frac{n}{N_d} \quad \text{Eq. 4}$$

Creep damage is calculated through the time fraction approach. The stress relaxation history is used to calculate the incremental creep damage following Equation 5.

$$d_c = \int_0^{t_h} \frac{dt}{T_d(\sigma(t), T)} \quad \text{Eq. 5}$$

The total creep damage is calculated by multiplying the creep damage per cycle with the design cycles n . The total creep-fatigue damage is evaluated against the material independent creep-fatigue damage envelope with the intersection point (0.2,0.2), as shown in Figure 4. The idea is to use a single damage envelope for all the materials for Class B evaluations.

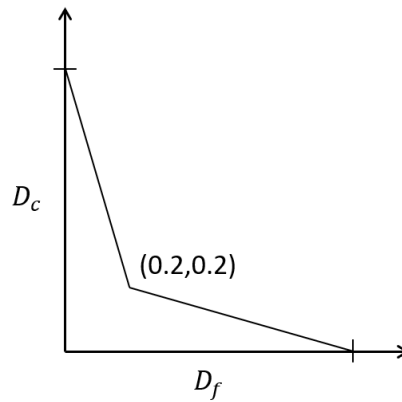


Figure 4. Material independent creep-fatigue damage envelope adopted with the intersection point of (0.2,0.2).

3. EVALUATION OF THE PROPOSED DESIGN-BY-ANALYSIS CREEP-FATIGUE METHODOLOGY

Components are designed for a selected design life based on designer's requirements. In this report, the performance of the proposed Class B code case is evaluated through the maximum allowable design cycles N_{max} . The N_{max} is the maximum cycle number attainable for selected component and load cycle, such that the creep and fatigue damage fractions satisfy the creep-fatigue damage envelope. Figure 5 shows the schematics of the maximum allowable design cycle. The red lines represent the damage envelope with (a_f, a_c) as the coordinates of the damage envelope intersection point. The blue line (Line A) is the damage slope for a given load cycle. Cycles required to reach the intersection of Line A and the damage envelope is the maximum allowable design cycles.

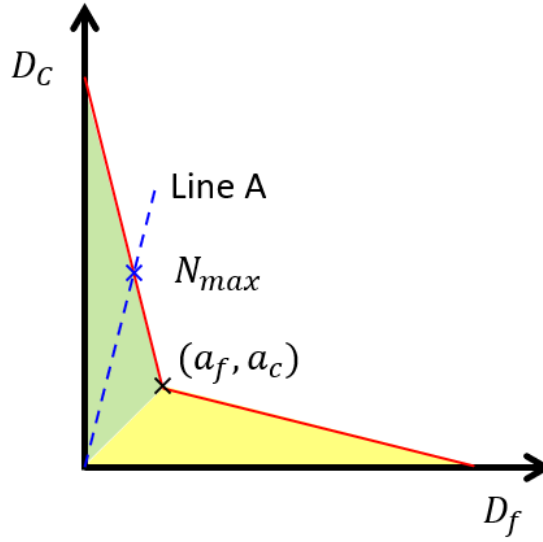


Figure 5. Schematic representation of creep and fatigue damage fractions for the maximum allowable design cycle, shown with Line A, compared against a generic creep-fatigue damage envelope.

The blue line represents the path of the creep-fatigue damage for a given component under load. The slope of the blue line is:

$$m = \frac{dD_c}{dD_f} \quad \text{Eq. 6}$$

where

dD_c = creep damage per cycle

dD_f = fatigue damage for one cycle $1/N_f$.

Using the general equation of the line and coordinates $(0, 1)$ and (a_f, a_c) , equation of the red line adjacent to the creep damage governed region (green region in Figure 5) is written in terms of the values of the creep damage y and the fatigue damage x as follows:

$$y = -\frac{1 - a_c}{a_c}x + 1 \quad \text{Eq. 7}$$

At the intersection point, the y and x in Equation 7 are creep and fatigue damage accumulated over maximum allowable design cycles N_{max} . Therefore, replacing x and y with the total fatigue and creep damage accumulated over N_{max} and rearranging Equation 7 yields Equation 8.

$$N_{max} = \frac{1}{dD_c + \frac{1-a_c}{a_c} dD_f} \quad \text{Eq. 8}$$

In Equation 8, creep damage per cycle is replaced in terms of fatigue damage using Equation 6. Thus, the maximum allowable design cycle for a creep damage governed regime ($m > \frac{a_f}{a_c}$) is given by Equation 9.

$$N_{max} = \frac{1}{dD_f \left[m + \frac{1-a_c}{a_c} \right]} \quad \text{Eq. 9}$$

If Line A is in the fatigue damage governed region (yellow region in Figure 5) with a slope smaller than $\frac{a_f}{a_c}$, the equation of the red line adjacent to the yellow region as shown in Figure 5, is given by Equation 10.

$$y = -\frac{a_f}{1-a_f}x + \frac{a_f}{1-a_f} \quad \text{Eq. 10}$$

Upon rearranging Equation 10 and replacing x and y with the fatigue and creep damage accumulated over N_{max} , respectively, Equation 11 is derived.

$$N_{max} = \frac{1}{dD_c \frac{1-a_f}{a_f} + dD_f} \quad \text{Eq. 11}$$

Replacing the creep damage over one cycle term by fatigue damage per Equation 6, Equation 12 provides the maximum allowable design cycle for fatigue damage governed regime ($m < \frac{a_f}{a_c}$).

$$N_{max} = \frac{1}{dD_f \left[m \frac{1-a_f}{a_f} + 1 \right]} \quad \text{Eq. 12}$$

Equation 9 and Equation 12 provide the maximum allowable design cycles for Class B methodology. The design cycles from these equations are compared against the Class A elastic analysis methodology to justify the validity of the proposed Class B rules. Note that Class A elastic analysis rules do not use the maximum allowable cycle definition. The Class A approach calculates the creep and fatigue damage for the specified number of cycles separately, and then the sum is compared against the Class A creep-fatigue damage envelope. The sum must be less than the damage interaction line.

To validate the proposed Class B design-by-analysis rules, a set of example problems are selected, as listed in Table 1. Although Class B does not rely on the stress classification, this table gives an overview of the selected components and respective stress classification of load cycles to be compared against the Class A elastic rules. Class B design-by-analysis rules propose to use an elastic follow-up of two ($q = 2$). This report presents results from Class B rules with elastic follow-up values of one and two. The Class B rules with $q = 1$ serves as a bounding case, as Class B with $q = 1$ results will always be less conservative compared to $q > 1$. The following subsections discuss an example problem with selected load conditions. All example problems in this report consist of a simple load cycle.

Table 1. A summary of an example problem with the respective load cycles.

Component	Primary Load*	Secondary Load*
Multiaxial Tube	Pressure	Cyclic end displacement load
Single Bar Simplified Model Test (SBSMT)	No	Cyclic end displacement load
Pressurized SBSMT (p-SBSMT)	Pressure	Cyclic end displacement load
Pressurized Simplified Model Test (p-SMT)	Pressure	Cyclic end displacement load
Bree Problem	Pressure	Temperature gradient across thickness
Flat Head Vessel	Pressure	Temperature gradient across thickness

* Stress classification is not needed for the new Class B rules but shows a key difference in the load cycles for different components. Stress classification is needed for Class A elastic design rules.

3.1 Multiaxial Isothermal Tube

Working towards the evaluation of the proposed Class B methodology, a uniform geometry with a simple load cycle was selected. Multiaxial isothermal tube experiments were conducted by Majumdar [5] on 316H straight-gauge geometry tubes. The specimen at 593°C was pressurized with a constant internal pressure of 7.58 MPa (1100 psi) and was subjected to a strain controlled by fully reversed cyclic axial loading with a strain range of 0.5%. The strain was held constant at peak tensile strain for one minute, resulting in an elastic follow-up of one. The failure cycle from the test was 3821. The maximum allowable design cycles calculated from the new Class B methodology are compared against the Class A elastic approach in Table 2.

Table 2. Maximum allowable cycles from Class A elastic compared against the Class B rules and failure cycles from multiaxial tube experiment.

Test results [5]			Class A Elastic		Class B ($q = 1$)		Class B ($q = 2$)	
q	$\Delta\epsilon$ (%)	Failure Cycles	$\Delta\epsilon$ (%)	N_{max}	$\Delta\epsilon$ (%)	N_{max}	$\Delta\epsilon$ (%)	N_{max}
1	0.5	3821	0.543	463	0.5	624	0.89	128

Similar to the Class A creep-fatigue evaluation procedure, the new Class B creep-fatigue design provision is also very conservative. The use of either $q = 1$ or $q = 2$ in the new Class B creep-fatigue design rules still leads to very conservative maximum allowable cycles as compared with the failure cycles from the test results. The results in Table 2 suggest that the use of an elastic follow-up of two ($q = 2$) is adequately conservative as compared with the Class A elastic method. The total strain range for the Class A elastic analysis method includes corrections due to the multiaxial stress state and the creep strain. For Class B with $q = 2$, the stress relaxation contributes to an additional strain accumulation, thus resulting in a higher total strain range that accounts for the elastic follow-up effect. This leads to a conservative fatigue damage fraction compared to the Class A elastic approach. Hence, for fatigue damage -dominated components, the proposed Class B approach is inherently conservative compared to the Class A elastic analysis approach. The only exception is for a load cycle at low temperatures and shorter cycle times, where the accumulated creep strain from the Class B methodology will be smaller compared to the Class A approach, which also accounts for the multiaxial stress state.

3.2 Single Bar Simplified Model Test

The Alloy 617 solid cylindrical SBSMT had a software-controlled test setup, resulting in the application of the desired strain range and a preselected elastic follow-up [6]. The strain range at the start of the test was 0.22%, and the experimentally measured elastic follow-up was three at 950°C. The failure cycle from this test was 4522. The proposed Class B method discussed in the previous section is used to calculate the creep-fatigue life. Table 3 lists the maximum allowable design, N_{max} , cycles from Class B with $q = 1$ and $q = 2$. The maximum allowable design cycles from different elastic follow-up values are about two orders of magnitude smaller compared to the failure cycles from the test. Note that the test data shows the strain range of SBSMT increases with time, which is not accounted explicitly in the Class B methodology. The bounding Class B analysis (Class B with $q = 1$) results in a conservative design life.

Table 3. Comparison of the maximum allowable design cycles from Class B against the failure cycles from the SBSMT experiment.

Failure Cycles [6]	Maximum allowable design cycles from Class B	
	$q = 1$	$q = 2$
4522	66	28

The stress-strain data of the first load cycle from the test is compared against the path followed by the Class B methodology in Figure 6a. The black line with a cross shows the material response. The dashed line connecting the origin to the peak stress, $2S_{alt}$, shows the elastically calculated stress range. Stress relaxes along the elastic follow-up line from peak stress to point ‘e’ along the dashed line. The material response considered for the design approach is shown in the solid red curve o-a-e, where the curve o-a is the hot tensile curve. Class B estimates a larger strain range compared to the test data, indicating conservative fatigue damage calculations. The stress relaxation profile of the first cycle the test results is compared against the stress relaxation profile from Class B in Figure 6b. Although the SBSMT test was conducted with $q = 3$, the proposed Class B methodology with $q = 2$ predicts higher stress intensities during stress relaxation. A higher total strain range and larger stress intensities during stress relaxation calculation from Class B with $q = 2$ ensure the conservatism of the proposed method against the failure data from the test.

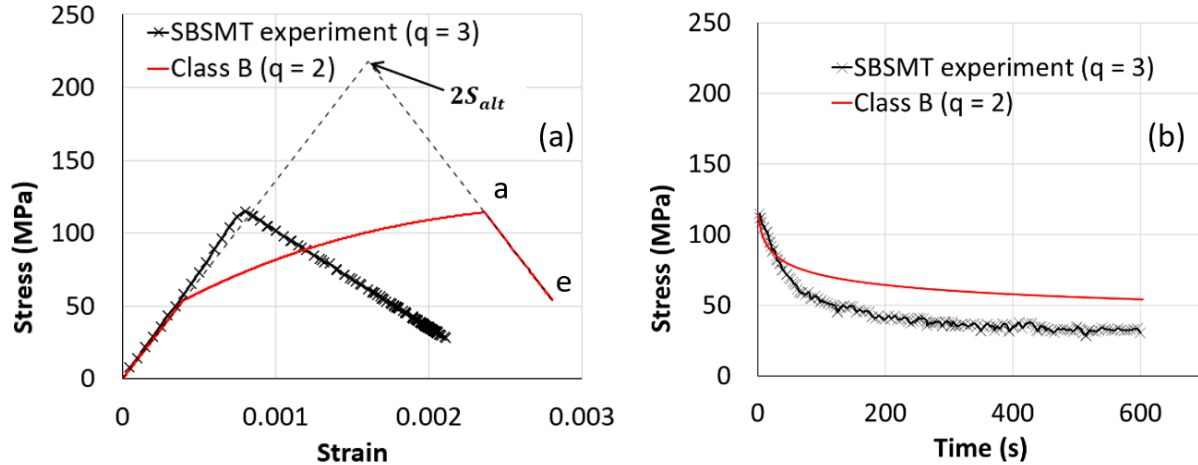


Figure 6. Comparison of (a) stress-strain data and (b) stress relaxation history from the Class B methodology against the SBSMT test data [6] from the first hysteresis loop until end of dwell time.

3.3 Pressurized Single Bar Simplified Model Test (p-SBSMT)

The tube-like SBSMT specimen fabricated with Alloy 617 was pressurized internally and subjected to hardware-contorted axial strain loading [7]. This setup applies the target strain range and elastic follow-up on the test specimen in addition to the internal pressure. Five load cases were selected with different internal pressures and target elastic follow-up values. These load cycles are evaluated against the proposed Class B methodology, and the maximum allowable design cycles are listed in Table 4. The cycle prediction from Class B bounding analyses ($q = 1$) consistently estimate an order of magnitude lower for the maximum allowable design cycles than the failure cycles from the tests. This suggests that the proposed Class B rules are conservative when compared against the failure cycles from the tests.

Table 4. Comparison of the failure cycles from the p-SBSMT experiment against the Class B maximum allowable design cycles for different load cases.

Experimental Data [7]						Class B Methodology		
Name	P (MPa)	q	$\Delta\epsilon$ (%)	Dwell Time (s)	Failure Cycles	$q = 1$	$q = 2$	$q = 6$
SBAP4	0.01	6.1	0.18	600	3641	88	43	10
SBAP5	1.03	3.4	0.53		201	28	11	2
SBAP6	0.01	3.53	0.53		347	28	11	2
SBAP9	1.03	1.96	0.28		996	149	85	24
SBAP7	0.01	2.02	0.25		3224	149	85	24

The stress-strain plots from Class B with $q = 6$ for test SBAP4 is compared in Figure 7a. The total strain range and stress intensities from Class B are consistently larger compared to the recorded test data, resulting in conservative fatigue and creep damage fraction calculations. Note that for this test, as the cycle progresses, stress values during relaxation phase drops with an increase in cycles. The blue cross in Figure 7b shows the stress relaxation history of the cycle 10. The proposed Class B uses $q = 6$ for cases with stress concentration regions; however, this comparison provides a basis to validate the proposed Class B rules against high elastic follow-up load cases. This comparison suggests the Class B rules are conservative for high elastic follow-up loads.

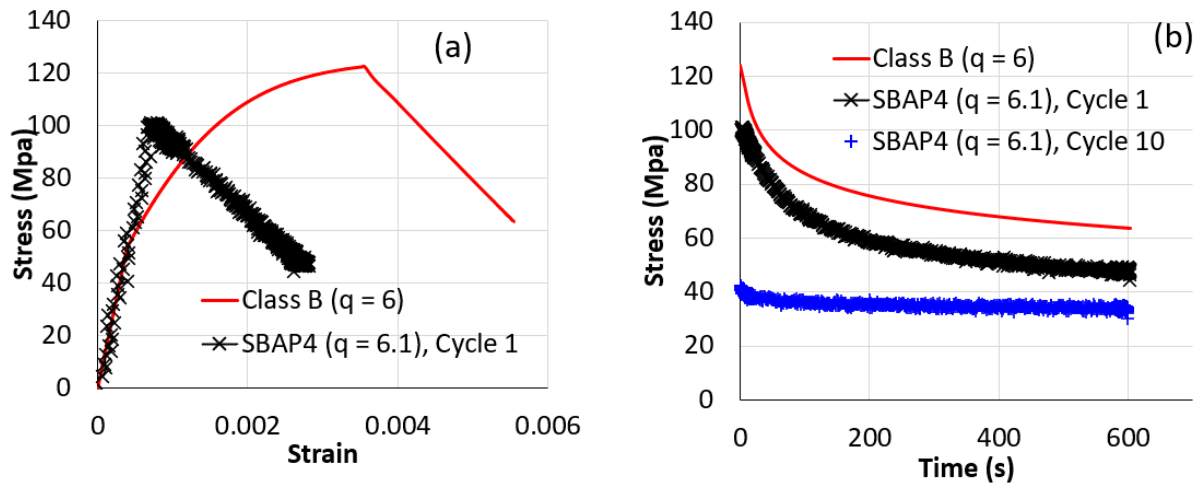


Figure 7. Comparison of (a) stress-strain data until the end of hold time and (b) stress relaxation history from the Class B with $q = 6$ against p-SBSMT test data SBAP4 [7].

Test SBAP5 with a follow-up of 3.4 was selected to compare against the Class B with $q = 2$ to check if Class B can capture test results with $q > 2$. The rationale behind this comparison is to check if the proposed Class B rules with $q = 2$ can capture components responses with a wider set of elastic follow-up values. The stress-strain comparison and the stress relaxation data are compared in Figure 8. This comparison shows the strain range from Class B ($q = 2$) is conservative compared to the test results with $q = 3.4$. The stress intensities at the start of the relaxation from the test are higher compared to the Class B methodology; however, stress intensities from the test relaxes with faster rates and stabilizes to lower stress values compared to the Class B stress predictions, as shown in Figure 8b, for the first and tenth cycle. This comparison shows the creep damage fraction from Class B is conservative compared to the test results.

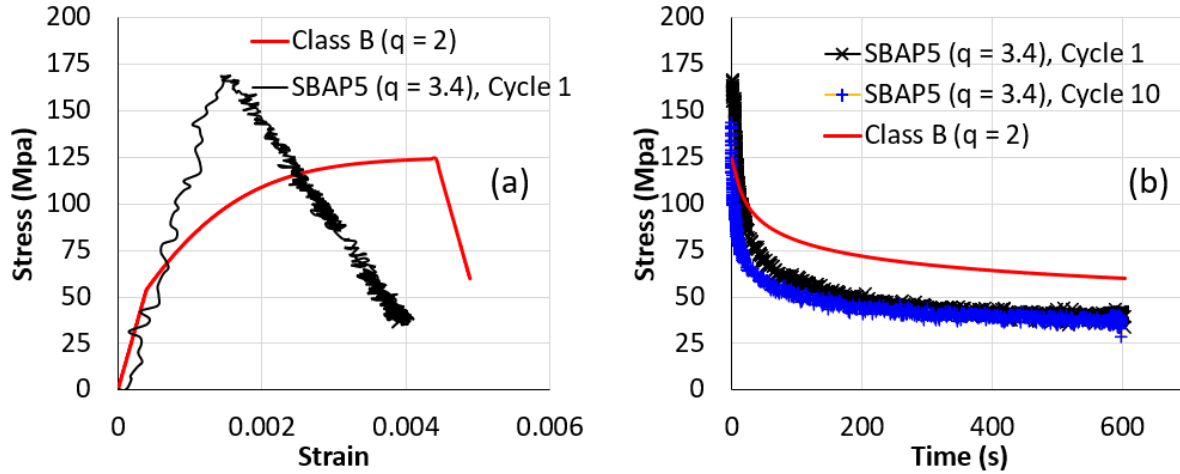


Figure 8. Comparison of (a) stress-strain data until end of hold time and (b) stress relaxation history from the Class B with $q = 6$ against p-SBSMT test data SBAP5 [7].

3.4 Pressurized Simplified Model Test (p-SMT)

A second example problem was the pressurized Simplified Model Test (p-SMT) specimen. The p-SMT test specimen was developed and tested to capture the realistic component behavior [8]. Figure 9 shows the geometry of the p-SMT specimen. An axisymmetric model with a quarter model symmetry captured the response of the p-SMT specimen. The internal volume of the specimen is pressurized, and the cyclic end displacements are applied such that the measured displacements at the 5-in. gauge length, shown in the Figure 9, matched with the target displacement range. This specimen had a reduced section at the center and had regions with higher thickness on both sides. This geometry was designed for an elastic follow-up greater than one. The test specimen was fabricated with Alloy 617 material and tested under an isothermal state. A total of six load cases were selected with different test temperatures (T) of 850°C and 950°C, externally applied displacement amplitude (δ), hold time (t_{dwell}), and internal pressure (P). The calculated elastic follow-up from the test data was in the range of 3.8 to 4. Hence, this test specimen provides a good baseline for the validation of the proposed Class B methodology for component.

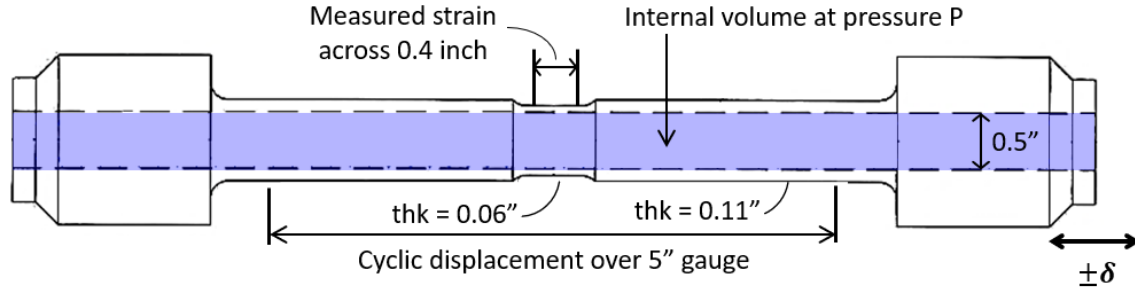


Figure 9. Specimen geometry of the pressurized SMT [8].

Table 5 compares the load details and the maximum allowable cycles from Class B against Class A elastic approach for different load cycles. This example problem validates the use of Class B rules with $q = 2$ against the test data with an elastic follow-up greater than 2. The design lives per Class B rules are consistently conservative compared to the test data. Although the maximum allowable design cycles from the proposed Class B ($q = 2$) are less conservative compared to Class A, an order of magnitude conservatism is observed between the Class B life prediction and the failure data from the tests.

Table 5. Comparison of the maximum allowable design cycles from Class A elastic and Class B design methodology against the failure cycles from p-SMT tests.

Load Case #	T (°C)	$\pm\delta$ (mm)	t_{dwell} (sec)		P (MPa)	Test data		N_{max}		
			Tensile	Comp		Failure Cycles	q	Class A Elastic	Class B ($q = 1$)	Class B ($q = 2$)
P01	950	0.1143	600	0	0.01	220	3.8	0	33	12
P05	950	0.1143	600	600	0.01	320	3.5	0	26	10
P02	950	0.1143	600	0	1.38	220	3.8	0	33	12
P12	950	0.0635	600	0	0.01	1360	4.1	3	82	39
P14	850	0.0762	600	0	2.76	3440	3.5	5	349	142
P15	850	0.0762	600	0	0.14	3460	3.5	6	349	142

3.5 Bree Problem

Conceptually, the Bree problem is comparable to the multiaxial tube discussed in the previous section, except the thermal gradient across thickness introduces axial stress gradients across thickness. Figure 10 shows the schematic of the Bree problem. The cross section is modeled as a series of elements with axial deformation constraints on the bottom nodes. The top nodes are constrained such that no shear deformations are allowed in elements. The elastic follow-up in this example problem is one due to the uniform geometry. The temperature load history shown in Figure 10b is applied to the inside and outside of diameter, referred as T_{ID} and T_{OD} , respectively. Dwell time, t_{dwell} , of 1,000 hours is selected. Alloy 617 and stainless steel 316H materials are selected as candidate material. A wide variety of load cases are selected for both materials. The maximum allowable design cycles from Class B with $q = 1$ and $q = 2$ are compared against the Class A elastic analysis methodology in Table 6.

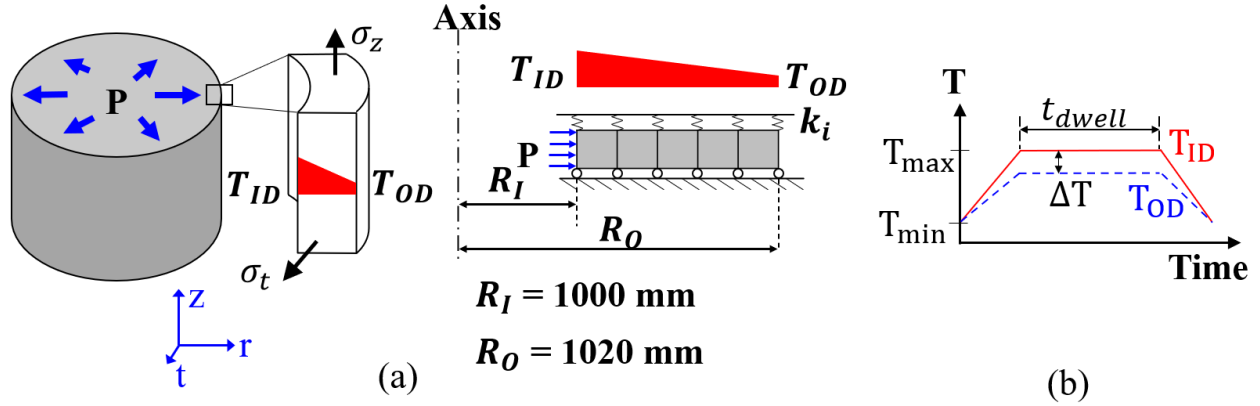


Figure 10. (a) Bree problem schematics with the boundary conditions and (b) temperature load profile.

The normalized lives from Class B with $q = 1$ and $q = 2$ are presented in Figure 11, where maximum allowable design cycles from Class B are divided by the maximum allowable design cycles from Class A elastic analysis approach. If this ratio is greater than one, Class A elastic is conservative compared to Class B, and vice versa. Load cases with higher creep damage accumulation rates at an elevated temperature for given material, shown with the green backgrounds, suggest Class B design cycles are comparable to Class A. For a lower temperature regime highlighted in the yellow background, increasing the temperature gradient across thickness results in a conservative estimation of the design cycles for 316H material. This difference is due to the primary creep influence on the Class A design life.

The creep damage per cycle calculated from Class A is compared against Class B in Figure 12. At 600°C, the primary creep accelerates the stress relaxation in the Class A ISSCs. Class B uses only secondary creep rates, resulting in a consistently higher estimation of stresses. This difference in stress relaxation histories results in smaller creep damage fractions from Class A compared to the Class B for the 316H material. Class A uses the safety factor for creep damage fraction calculation, where stresses are divided by K' factor ($K' = 0.9$ for 316H and Alloy 617). Current Class B rules do not use any factor on stresses, yielding smaller creep damage fractions from Class B ($q = 1$) when compared to the Class A elastic approach. The comparison results do not suggest the need for the K' factor for Class B rules.

Table 6. Maximum allowable design cycles comparison from proposed Class B against the Class A Elastic calculated from the creep-fatigue damage.

Load Case #	Material	T_{max} (°C)	P (MPa)	ΔT (°C)	N_{max}		
					Class A Elastic	Class B ($q = 1$)	Class B ($q = 2$)
1	316H	700	0	9.4	722	1073	959
2				18.7	105	193	126
3				46.8	5	35	12
4			0.11	9.4	718	813	697
5				18.7	106	168	107
6				46.8	5	34	11
7			0.23	9.4	715	630	517
8				18.7	105	148	92
9				46.8	5	33	10
10		600	0	9.9	15384	18356	18337

Load Case #	Material	T_{max} (°C)	P (MPa)	ΔT (°C)	N_{max}		
					Class A Elastic	Class B ($q = 1$)	Class B ($q = 2$)
11				19.8	5434	3620	3533
12				49.4	464	99	65
13				9.9	14925	14920	14893
14			0.11	19.8	5376	2982	2890
15				49.4	458	89	59
16				9.9	14493	12136	12100
17			0.23	19.8	5348	2464	2368
18				49.4	453	82	53
41				12.1	76	107	78
42	Alloy 617	900	0	24.2	15	12	10
43				60.5	0	1	0
44				12.1	80	82	61
45			0.13	24.2	15	10	8
46				60.5	0	0	0
47				12.1	59	63	48
48			0.26	24.2	15	9	7
49				60.5	0	0	0
50		800	0	12.1	212	330	270
51				24.2	10	76	55
52				60.5	0	1	1
53			0.13	12.1	203	259	203
54				24.2	9	66	48
55				60.5	0	1	1
56			0.26	12.1	195	209	159
57				24.2	9	57	42
58				60.5	0	1	1

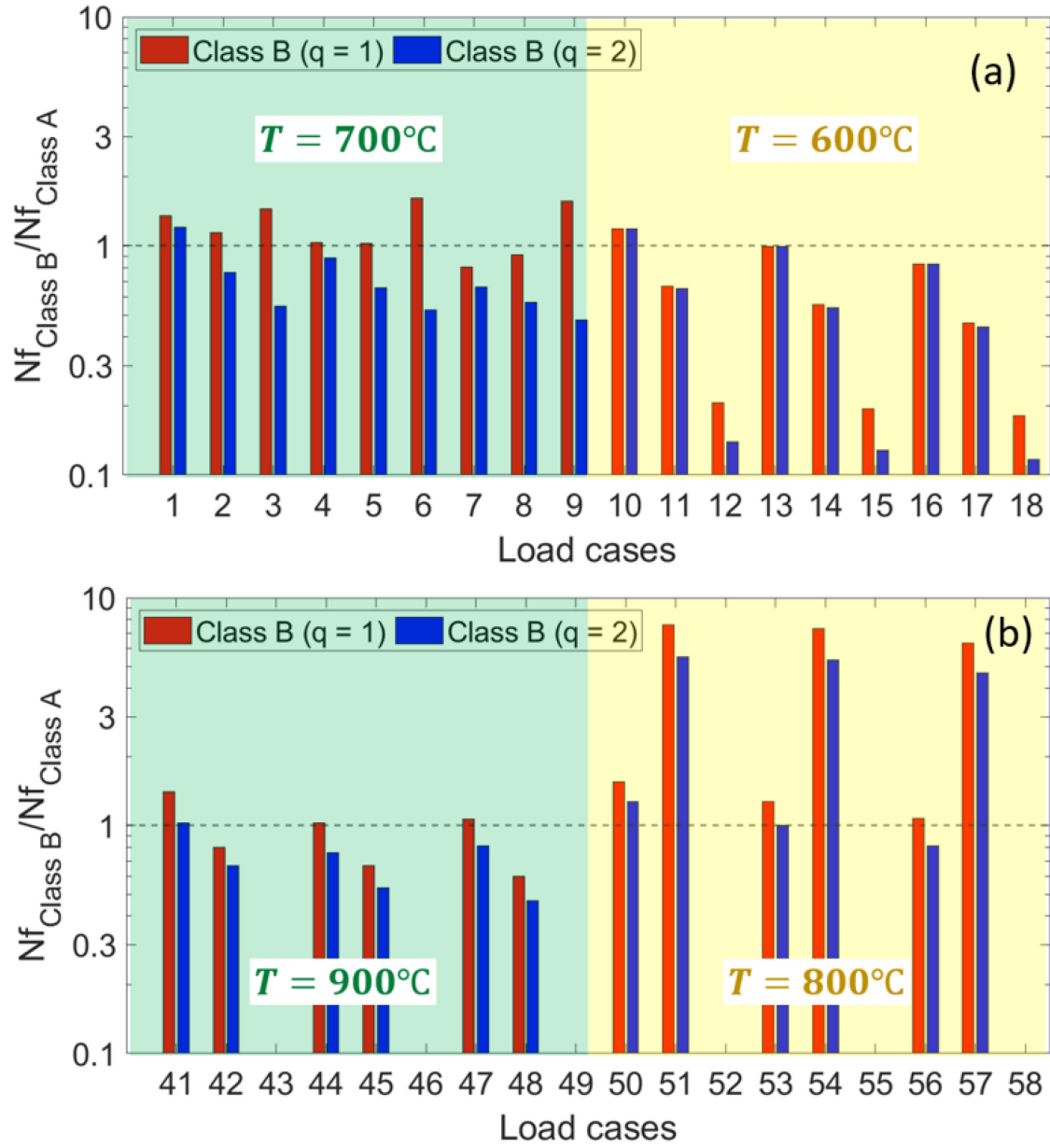


Figure 21. Normalized life comparison calculated by dividing the maximum design cycles from Class B by the design cycles from Class A elastic rules for the Bree problem with different load cases for (a) 316H and (b) Alloy 617.

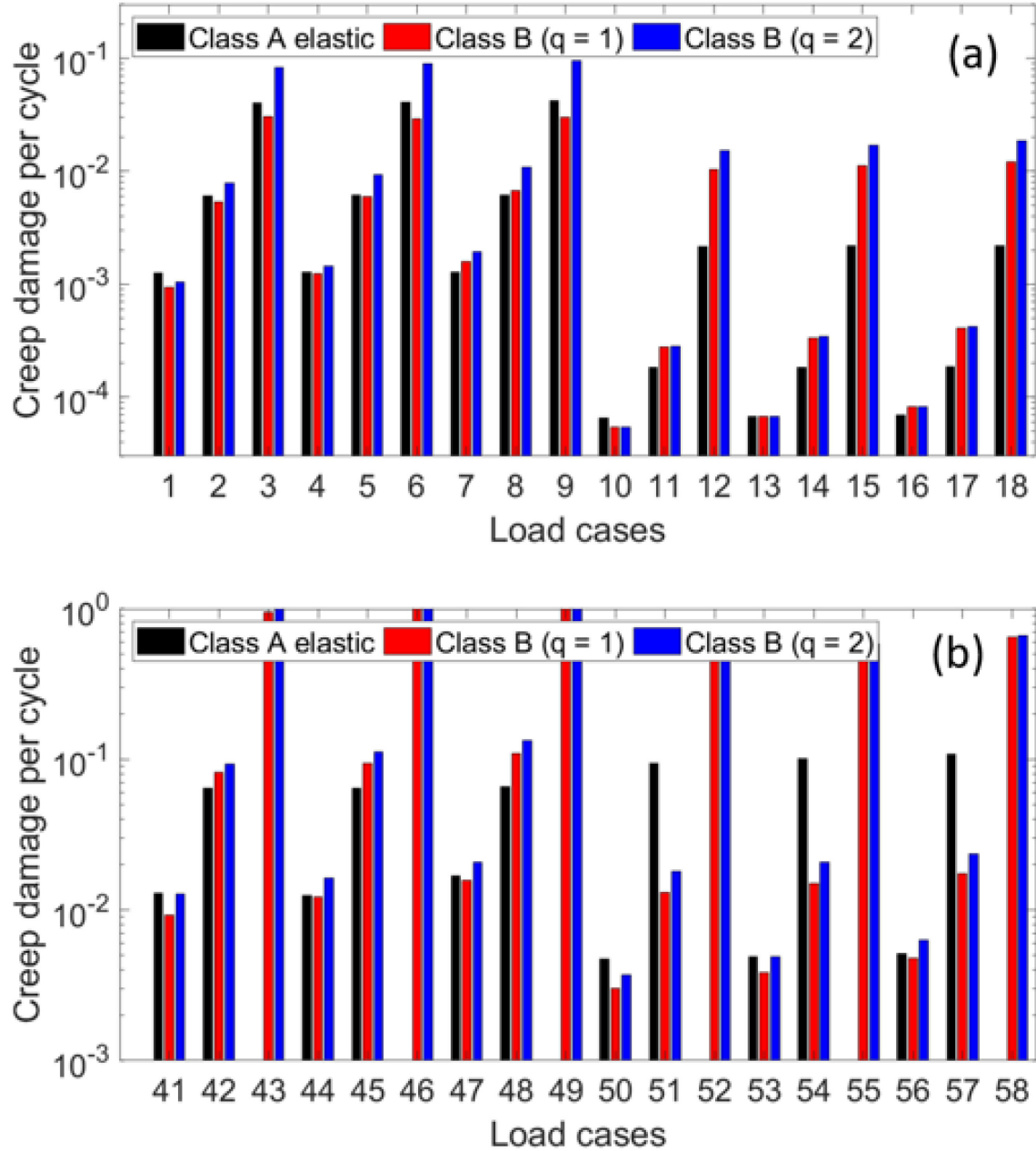


Figure 3. Creep damage accumulated over one cycle from Class A elastic and Class B methodologies for the Bree problem with different load cases for (a) 316H and (b) Alloy 617.

3.6 Flat Head Vessel

A flat head vessel (FHV) geometry is selected, as shown in Figure 13. The knuckle in the FHV was modeled with a corner radius of 6.35 mm (0.25 inch). The temperature cycle for the inside dimension (ID) is shown in red and the outside dimensions (OD) is shown in blue. The ID temperature is always higher compared to OD. The maximum temperature gradient across thickness was selected as 20°C during the dwell. The vessel was pressurized with a constant pressure of 0.1 MPa. The selected loads represent a typical load cycle observed for molten salt reactors [9]. Different dwell times were selected from 10 hours to 10,000 hours and the rest of the load cycle was kept identical for all load cases. In this example

problem, 316H material is selected as a candidate material. The stress concentration factor at the knuckle is 1.46.

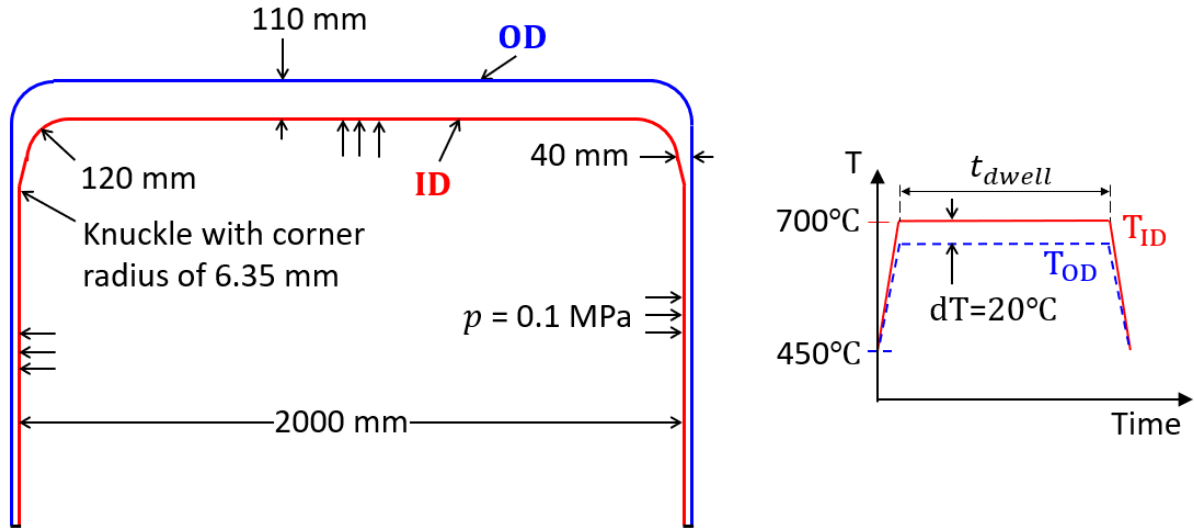


Figure 4. FHV geometry with the temperature load history.

The maximum allowable cycles from Class A elastic and Class B rules are compared in Table 7. The Class A total strain range for fatigue damage calculation is compared against the strain range from Class B in Figure 14. This comparison shows the ability of Class B to capture the effects of the elastic follow-up on the fatigue damage fraction.

Table 7. Comparison of maximum allowable design cycles from Class A and Class B.

ID	t_{dwell} (hr)	N_{max} Class A Elastic	N_{max} from Class B	
			$q = 1$	$q = 2$
1	10	312	54	35
2	30	127	37	23
3	100	47	25	15
4	300	18	17	10
5	1000	6	9	6
6	3000	2	4	3
7	10000	0	1	1

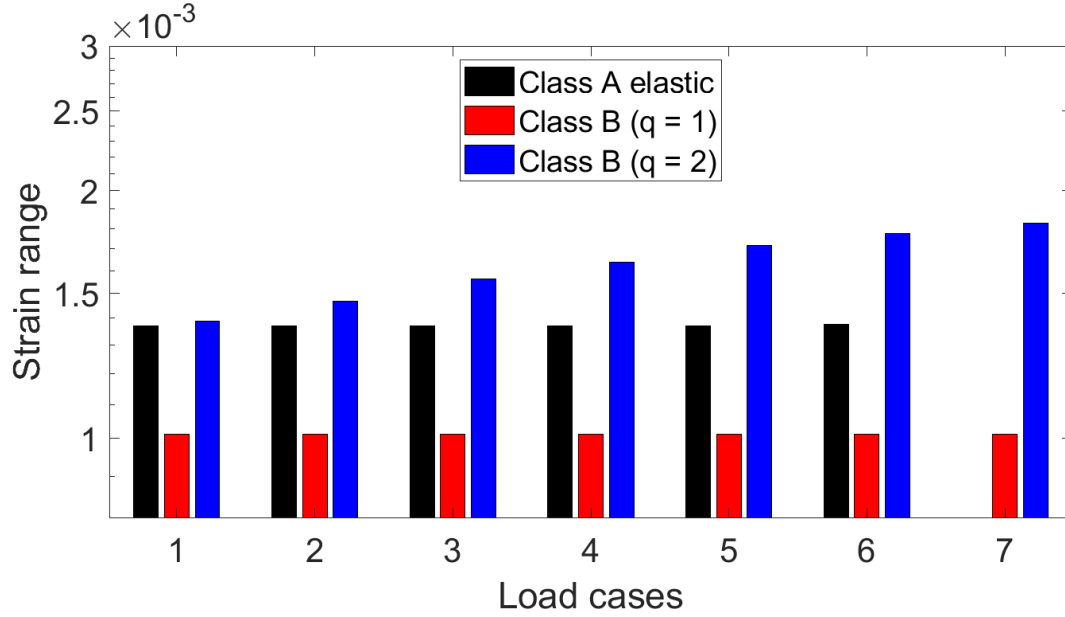


Figure 5. The total strain ranges from Class A elastic and Class B methodologies for FHV problem with different load cases.

The creep damage per cycles from Class A and Class B are compared in Figure 15. The Class A design rules use primary and secondary creep rates, resulting in a faster relaxation of stresses affecting the lower creep damage per cycle. This results in a larger design life for shorter dwell times. As dwell time is increased, the influence of the primary creep starts to diminish as the secondary creep rates from Class B start to relax. Hence, with an increase in dwell time beyond 100 hours, life estimation from Class B bounding analysis ($q = 1$) approaches the design life predictions from Class A elastic design rules.

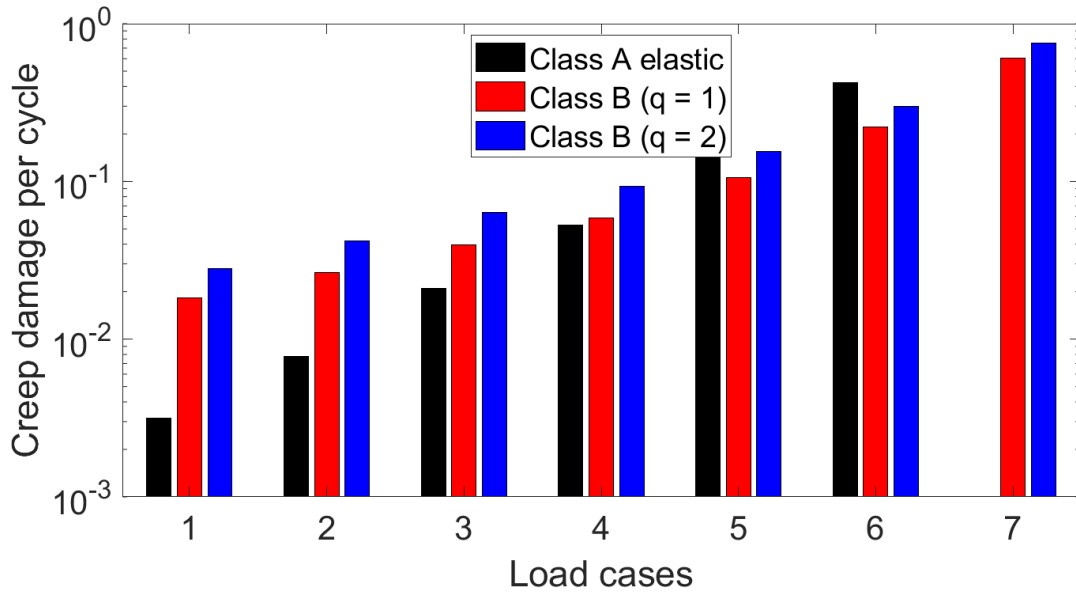


Figure 6. Creep damage accumulated over one cycle from Class A elastic and Class B methodologies for FHV problem with different load cases.

3.7 Influence of Primary Creep on the Class B Methodology

This subsection evaluates the influence of primary creep in the ISSCs for the new Class B methodology. The maximum allowable design cycles from Class B are calculated by using (a) the standard ISSCs that include primary creep, if present, and secondary creep and (b) the simplified ISSCs that only include secondary creep. They are compared against the design cycles from Class A elastic rules.

The standard ISSCs give higher strain rates as compared with the simplified ISSCs. This leads to faster stress relaxation during the dwell time, lower creep damage, and higher allowable design cycles. Alloy 617 is an example of a Class A material that only has secondary creep in the ISSCs. The material chosen for the comparison is 316H stainless steel because it has both primary and secondary creep in the standard ISSCs.

The multiaxial isothermal tube response is governed by the fatigue damage, meaning this test has lower influence of creep on the failure cycles from the tests. The maximum allowable design cycles calculated by using primary and secondary creep was identical when compared against life calculated using only secondary creep. For this component, the effect of introducing the primary creep is very small as this is a fatigue damage governed load case with a test temperature of 593°C and a short dwell time.

For the Bree problem, both standard and simplified ISSCs are used in the new Class B methodology, and the resulting maximum allowable design cycles, together with those from the Class A elastic analysis, are compared in Table 8.

Table 8. Influence of the primary creep strain on the design cycles for the Bree problem.

Load case #	ΔT (°C)	Class A Elastic N_{max}	N_{max} Calculated from Class B Rules			
			Using Simplified ISSCs		Using Standard ISSCs	
			$q = 1$	$q = 2$	$q = 1$	$q = 2$
1	9.4	722	1073	959	1728	1433
2	18.7	105	193	126	532	370
3	46.8	5	35	12	29	25
4	9.4	718	813	697	1444	1160
5	18.7	106	168	107	472	326
6	46.8	5	34	11	26	22
7	9.4	715	630	517	1223	955
8	18.7	105	148	92	421	289
9	46.8	5	33	10	24	21
10	9.9	15384	18356	18337	18594	18460
11	19.8	5434	3620	3533	4417	4010
12	49.4	464	99	65	319	205
13	9.9	14925	14920	14893	15245	15063
14	19.8	5376	2982	2890	3794	3384
15	49.4	458	89	59	297	189
16	9.9	14493	12136	12100	12553	12322
17	19.8	5348	2464	2368	3278	2871
18	49.4	453	82	53	278	175

The standard ISSCs that include primary creep led to higher maximum allowable design cycles. This increase is dominant at 600°C, where primary creep affects the ISSCs significantly as compared to 700°C. Figure 16 shows the comparison of the creep damage accumulated in one cycle from Class B ($q = 2$) using the simplified and standard ISSCs.

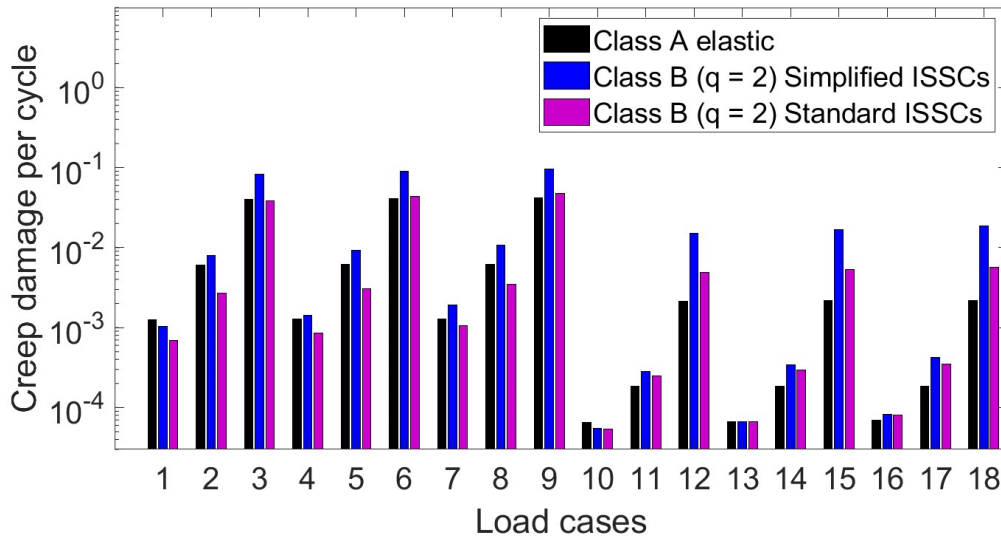


Figure 76. Creep damage accumulated over one cycle from Class A elastic and Class B methodologies using the simplified ISSCs and the standard ISSCs for the Bree problem with different load cases.

Class B maximum allowable design cycle ratios against those of Class A are calculated and presented in Figure 17. If the ratio is greater than one, the Class B rules are less conservative compared to Class A elastic design rules. Note that this ratio is plotted in the logarithmic scale. The presence of primary creep in the standard ISSCs results in the net increase in the predicted maximum allowable design cycles as compared to the simplified ISSCs when using the new Class B rules. The primary creep affected the load cases at 600°C with higher thermal gradient across thickness (load case # 12, 16, 18.)

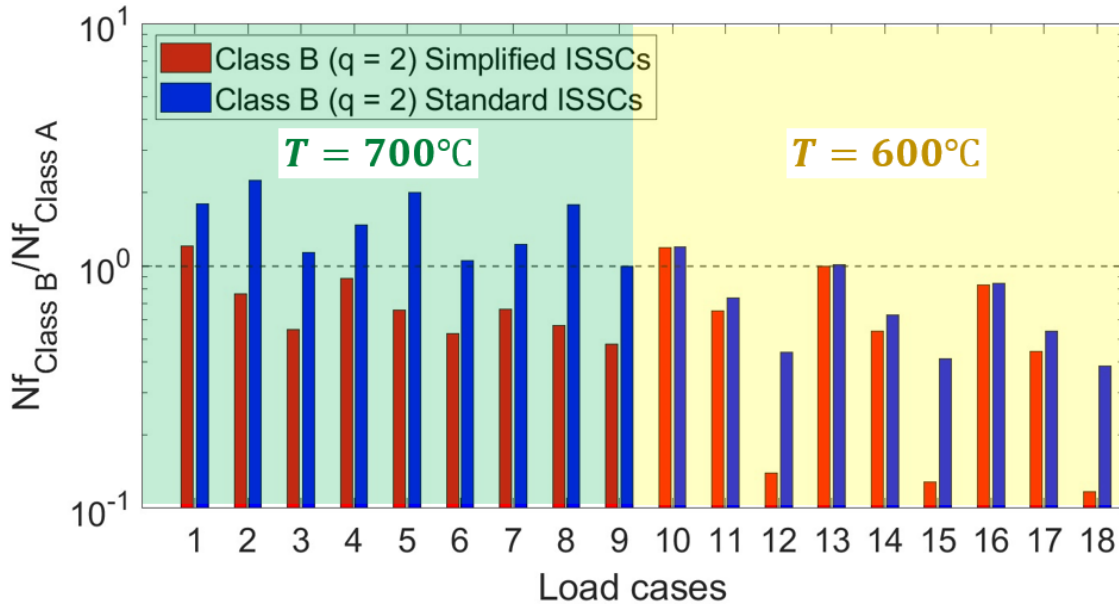


Figure 8. Influence of the primary creep on the normalized life for the Bree problem with different load cases.

The Table 9 compares the maximum allowable design cycles for FHV from Class B with simplified and standard ISSCs. For the $q = 2$, using primary creep consistently yielded higher design life for a dwell

time of more than 30 hours. The creep damage accumulated in one cycle for Class B ($q = 2$) methodologies is compared in Figure 18. For dwell times above 30 hours, the introducing primary creep results in lower creep damage per cycle. The typical hold times in components are more than 30 hours, which suggests the proposed Class B methodology with $q = 2$ and primary and secondary creep would result in a higher maximum allowable design cycle compared to the Class A elastic design rules.

Table 9. Influence of the primary creep strain on the design cycles for FHV.

Load Case #	t_{dwell} (hr)	N_{max} from Class A Elastic	N_{max} from Class B			
			Using Simplified ISSCs		Using Standard ISSCs	
			$q = 1$	$q = 2$	$q = 1$	$q = 2$
1	10	312	54	35	204	122
2	30	127	37	23	144	87
3	100	47	25	15	84	54
4	300	18	17	10	42	30
5	1000	6	9	6	16	12
6	3000	2	4	3	5	4
7	10000	0	1	1	1	1

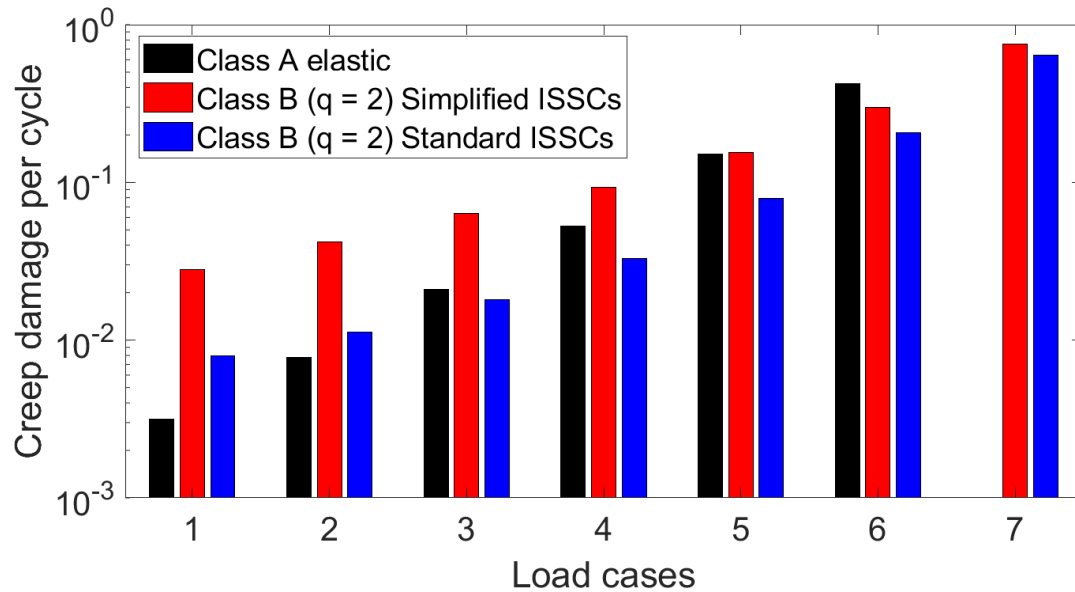


Figure 9. Creep damage accumulated over one cycle from Class A elastic and Class B methodologies with simplified and standard ISSCs for FHV problem with different load cases.

These comparisons show the influence of primary creep on the maximum allowable design cycles predictions for the new Class B rules.

4. CANDIDATE CLASS B MATERIALS

The candidate materials list has been identified for incorporation into the new Class B code case, as shown in Table 10. This list is sorted into three categories.

Table 10. List of candidate materials identified for incorporation into the new Class B code case.

First Category	Second Category	Third Category
Design data available from Section III Division 5 [2]	Creep data available from Section II, Part D, Tables 1A and 1B [10] (Non-Nuclear Applications)	Materials not in Section II, Part D, Tables 1A and 1B nor in Section III, Division 5
304H 316H Alloy 800H Grade 22 (solution annealed) Grade 91 Alloy 617	316L, 316Ti, Ti-mod 304 (TP321), 304N, 316N Alloy 690, Hastelloy X, Alloy 625, Hastelloy N, Haynes 230, Haynes 242, Haynes 282, Inconel 740H Grade 92, Grade 22 (N&T)	Alloy 709 XM-19 (NITRONIC 50) Haynes 244 HT-9 15-15-Ti XM-19

The first category has six materials as shown in the first column. These six materials are the Class A materials in Section III, Division 5. There are extensive databases for these materials, and they are sufficient to develop allowable stresses and design parameters for the new Class B code case.

The second category shown in Table 10 consists of austenitic stainless steels, nickel alloys, and high alloy steels. Allowable stresses for the materials in this category are listed in Section II, Part D, Tables 1A and 1B [10], and they are based on creep rupture and minimum creep rate data. There is not cyclic data or creep rupture data for weldments. Cyclic data are required to support the creep-fatigue evaluation of the new Class B code case, and weld creep rupture data are required for the primary load check for welded Class B construction. These are the data gaps for the materials listed under the second category.

Materials in the third category of Table 10 are not listed either in Section II, Part D, Tables 1A and 1B, or in Section III, Division 5. Alloy 709 is currently being qualified by the U.S. Department of Energy's Office of Nuclear Energy's Advanced Reactor Technologies Program. Data for the new Class B rules will be available upon the completion of the first Alloy 709 Class A code case. For the remaining materials in the third category, no data have been identified. Tensile, creep, fatigue, and creep-fatigue data of the base metal and creep rupture data of the weldment are necessary to generate the design parameters for the new Class B rules.

5. SUMMARY AND FUTURE WORK

The proposed design-by-analysis Class B rules are presented for strain limits evaluation and creep-fatigue damage assessment. The creep-fatigue rules capture the creep-fatigue performance of the materials through a new elastic follow-up-based ISSC relaxation procedure. These rules address current gaps in the Class B design methodology for elevated temperature applications.

The Class B creep-fatigue damage assessment by design-by-analysis rules were evaluated with experimental results and a set of sample problems. The maximum allowable design cycles from the Class B methodology were conservative compared to the experimental results by an order of magnitude. This comparison established the conservatism of the proposed Class B rules against the failure data from the tests. Similarly, the SBSMT, p-SBSMT, and p-SMT were evaluated using $q = 2$ in the Class B methodology. The maximum design cycles from the Class B approach were consistently more conservative by an order of magnitude compared to the experimental results. The Class B design life comparisons against experimental data support the use of $q = 2$. These comparisons also support the use of a universal creep-fatigue damage envelope with an intersection point of (0.2, 0.2).

The use of simplified ISSCs instead of the standard ISSCs in the new Class B design rules was assessed. The maximum allowable design cycles from the Class B rules using both ISSCs for 316H stainless steel, together with those from the Class A elastic method, were compared for the Bree problem with different load cases. Comparisons were also made for the sample problem of a FHV with a shorter dwell time. These comparisons showed that the use of the simplified ISSCs that only include secondary creep results in a more conservative estimate of the creep damage fraction compared to estimates using the standard ISSCs. The data that support the determination of the allowable stresses in ASME BPVC Section II, Part D, Tables 1A and 1B, only include the minimum creep rate data, which can be used to establish the simplified ISSCs but not the standard ISSCs. Thus, the use of the standard ISSCs in the new Class B design rules would significantly increase the data requirement for the Class B materials.

The candidate Class B materials list is presented, and data gaps are identified for these materials.

In the next FY, further assessments of the new Class B design rules will be made. Design parameters for some of the materials in the candidate Class B materials list that have adequate datasets will be developed. The design-by-analysis strain limits procedure will be evaluated using sample problems. Problems where the components have a high stress concentration will be selected to assess the new Class B rules for components with stress raisers. A composite cycle will be defined for selected sample problems, and the predictions from the new Class B rules will be compared against those from the Class A elastic, Class A EPP, and full inelastic analysis procedures.

REFERENCE

- [1] American Society of Mechanical Engineers (ASME) International. 2023. “Section III, Rules for Construction of Nuclear Facility Components, Division 5, High Temperature Reactors.” in ASME Boiler and Pressure Vessel Code: An International Code. New York, NY.
- [2] Sham, T-L., Wang, Y., and Mahajan, H. P. 2022. “Initial Development of Variable Design Lifetimes and Creep-Fatigue Evaluations for ASME Section III, Division 5, Class B Code Rules.” INL/RPT-22-69139, Idaho National Laboratory (INL), Idaho Falls, ID.
- [3] American Society of Mechanical Engineers (ASME) International. 2023. “Code Cases, Boilers and Pressure Vessels.” in ASME Boiler and Pressure Vessel Code: An International Code. New York, NY.
- [4] American Society of Mechanical Engineers (ASME) International. 2023. “Section III, Rules for Construction of Nuclear Facility Components, Appendices.” in ASME Boiler and Pressure Vessel Code: An International Code. New York, NY.
- [5] Majumdar, S. 1979. “Biaxial Creep-Fatigue Behavior of Type 316H Stainless Steel Tube.” No. ANL-79-33. Argonne National Laboratory (ANL), Argonne, IL (United States).
- [6] Mahajan, H. P., and McMurtrey, M. D. 2022. “Single-Bar SMT Creep-Fatigue Testing on Alloy 617 with Software Controls on Elastic Follow-Up Feedback in Support of New Creep-Fatigue Design Methodology.” INL/RPT-22-68896, Idaho National Laboratory (INL), Idaho Falls, ID.
- [7] Wang, Y., et al., 2020. “Report on FY2020 Test Results in Support of the Development of EPP Plus SMT Design Method.” ORNL/TM-2020/1620, Oak Ridge National Laboratory (ORNL), Oak Ridge, TN.
- [8] Wang, Y., et al. 2019. “Report on FY19 Testing in Support of Integrated EPP-SMT Design Methods Development.” ORNL/TM-2019/1224, Oak Ridge National Laboratory (ORNL), Oak Ridge, TN.
- [9] Koo, G.H., et al. 2023. “A Study on Creep-Fatigue Evaluation of Nuclear Cladded Components by ASME-III Division 5.” *Energies* 16 (6): 2898.
- [10] American Society of Mechanical Engineers (ASME) International. 2023. “Section II, Materials Properties,” in ASME Boiler and Pressure Vessel Code: An International Code.” New York, NY.